Hot Electron Spectra in Plain, Cone and Integrated Targets for FIREX-I using Electron Spectrometer*)

Tetsuo OZAKI, Hiroyuki SHIRAGA[1)], Yasunobu ARIKAWA[1)], Shinsuke FUJIOKA[1)], Hitoshi SAKAGAMI, Zhe ZHANG[1)], Atsushi SUNAHARA[1)], Hideo NAGATOMO[1)], Tomoyuki JOHZAKI[2)], Takuya NAMIMOTO[1)], Masaki TAGA[1)], Sadaoki KOJIMA[1)], Yuuki ABE[1)], Kazuhiro ISHIHARA[1)], Takahiro NAGAI[1)], Shohei SAKATA[1)], Shoji HATTORI[1)], Yohichi SAKAWA[1)], Hiroaki NISHIMURA[1)], Hiroshi AZECHI[1)] and FIREX GROUP[1)]

National Institute for Fusion Science, 322-6 Oroshi, Toki, Gifu 509-5292, Japan
[1)]*Institute of Laser Engineering, Osaka University, 2-6 Yamada-Oka, Suita, Osaka 565-0871, Japan*
[2)]*Graduate school of Engineering, Hiroshima University, 1-4-1 Kagamiyama, Higashi-Hiroshima 739-8527, Japan*

(Received 1 December 2012 / Accepted 5 April 2013)

The traditional fast ignition scheme is that a compressed core created by an imploding laser is auxiliary heated and ignited by the hot electrons (produced by a short pulse laser guided through the cone). Here, the most suitable target design for fast ignition can be searched for by comparison of the spectra between varied targets using an electron spectrometer.

Keywords: ESM, hot electron, FIREX, GXII, LFEX, cone, DLC, CD-shell, laser induced magnetic field, neutron

DOI: 10.1585/pfr.8.2404125

1. Introduction

Fast ignition (FI) [1–3] will be performed as follows; An imploded core with a density of several hundred times the solid density is created by an imploding laser. The imploding core is auxiliary heated and ignited by hot electrons. The hot electrons are produced by the interaction between a chirped ultra-short pulse laser and the pre-formed plasma created by the pre-pulse of the heating laser at the tip of a guiding cone. According to the simulation, the maximum coupling efficiency between the core and the hot electrons can be expected at the typical hot electron energy of 2 MeV or less [4]. Usually if the scale length (1/e-hold length) of the plasma density is long, the effective electron temperature T_{eff} (= slope of the electron spectrum) is high and the coupling efficiency is reduced because the electron passes through the core with small energy deposition. The low energy electron, which is suitable for FI, is reduced because most of the laser energy is expended for the creation of super energetic electrons. In many cases, T_{eff} becomes high because the scale length of the pre-formed plasma is longer than the expected value due to low laser contrast (main pulse/ pre-pulse ratio). Therefore it is one of the most important issues for FI that T_{eff} remains low with high laser to electron conversion efficiency.

Escaped hot electron spectra can be observed 1 m from the target by using an electron spectrometer (ESM) [5] based on a permanent magnet and an imaging plate. Only the tail component of the hot electron energy distribution can be observed because the escaped electron is affected by a target potential.

In this paper, the difference of T_{eff} in varied targets, which are measured by ESM, are shown. The behavior of the hot electrons in different targets is described. The most suitable target for FI is sought from T_{eff}, the electron flux and neutron yield.

2. Experimental Setup

The experimental setup is shown in Fig. 1. Gekko XII (GXII, 9-12 beams, 250 J/beam, 0.53 μmϕ, 2ω) [6] is used for implosion of the deuterated polystyrene shell (500 μmϕ, 7 μm thickness) with the cone. The LFEX laser (two beams, 1.053 μm) [7] energy is from 500 J to 1.6 kJ. The pulse width is 1.5 ps in experiments. The energy of 82% is focused at the focal spot size (50%) of 40 - 100 μmϕ.

We used three different type targets of plain, cone and cone-shell listed in Table 1. The time history of the shape and the trajectory of the imploding core and the cone (outer and inner) can be observed by MIXS [8]. The interaction between the cone inner and the laser can be seen by using a DLC (diamond-like-carbon)-cone [9] which is optically thin. The γn-neutron flux produced by the interaction between the strong x-ray and the target or the surrounding components (a target chamber) can be reduced in a DLC-cone. DD-neutrons are monitored by MANDALA [10] with a strong γn-neutron shield (collimated lead and polyethylene).

author's e-mail: ozaki@nifs.ac.jp
*) This article is based on the presentation at the 22nd International Toki Conference (ITC22).

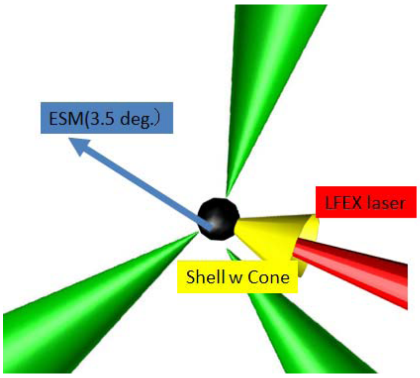

Fig. 1 Experimental setup. Shell with cone is imploded by the green laser. Imploded core is auxiliary heated by the hot electron created by the interaction between the LFEX laser and the cone tip. Escaped hot electrons are measured by ESM.

Table 1 Targets in FI01.

Plate
Aluminum, Copper (Cu), Gold (Au)
Cone
Gold cone
DLC w/wo Au-coat
Fundamental experiments (with imploding plasma)
Au-cone + semi-sphere CD shell + Ta/Cu-1mm^t
W-cone + semi-sphere CD shell + Ta/Cu-1mm^t
Open hole Au-cone + semi-sphere CD shell + Ta/Cu-1mm^t
DLC-cone + semi-sphere CD shell + Ta/Cu-1mm^t
Integrated experiments
Au-cone + Imploded core
DLC-cone + Imploded core
Open hole Au-cone + Imploded core
Open hole DLC-cone + Imploded core
B_{ext} application
Open hole-shell + B_{ext} + Imploded core
DLC-cone + B_{ext} + Imploded core

The calibrated ESM is installed on the GXII target chamber I at 3.5 degrees (port number 53) against the laser forward direction where it is almost at the rear side of the target but slightly oblique.

3. Comparison of the Spectra between Various Targets

The LFEX laser irradiates plain targets to measure the spot size and tuning diagnostics. We can compare the difference of the pre-formed plasma shape in varied materials. T_{eff} defined from the slope of the electron spectrum strongly depends on the scale length of the pre-formed plasma, which is mainly produced by the pre-pulse and/or the pedestal of the LFEX laser. According to Phukov scaling [11] obtained by simulation, the relation between T_{eff} and the scale length is as follows;

$$T_{eff} \sim 0.423(I/I_{18})^{(1/2)}(2.465L^{(1/4)} - 2.223), \qquad (1)$$

where I, I_{18} and L are the laser intensity in W/cm^2, the normalized factor of 10^{18} and the scale length in μm, respectively. All T_{eff} data dependence on LFEX laser intensity in this experimental series FI01 are shown in Fig. 2.

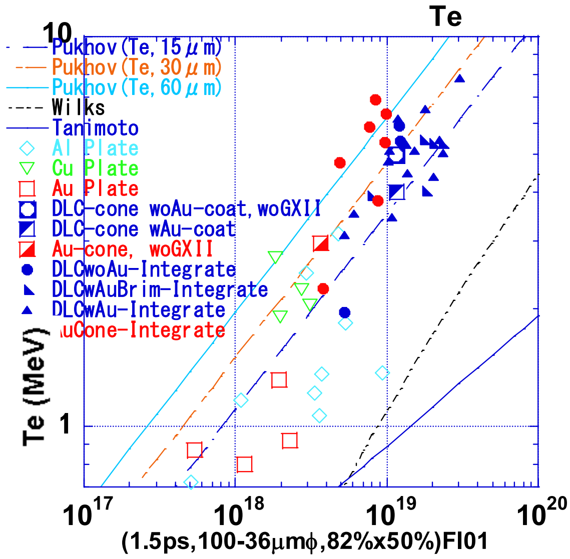

Fig. 2 Teff in FI01. T_{eff} can be obtained from the slope of the hot electron spectrum. Open, half open and closed symbols show the plain, the cone-only and the integrated targets, respectively. Tanimoto and Wilks scalings come from reference [15, 16].

3.1 Plain and cone targets

Generally T_{eff} becomes low when the target Z is large [12]. The pre-formed plasma of high-Z does not expand easily because the target mass number $A(\propto Z)$ is large. However T_{eff} in a copper target is much higher than T_{eff} in an aluminum one. One possibility is that the pre-formed plasma contains water on the copper surface.

We compare T_{eff} in a cone irradiated by the LFEX laser with T_{eff} in a plate. T_{eff} in the cone is obviously higher than T_{eff} in the plate. Several reasons can be considered. The pre-formed plasma in the cone converges to the cone axis which is the path of the LFEX laser. The effective pass length of the laser in the pre-formed plasma becomes long due to the geometrical effect of the expansion of the pre-formed plasma in the cone [13]. According to the simulation, the oblique injection of the laser makes the higher T_{eff} [14].

3.2 Integrated experiments

In the integrated experiments, the DLC-cone is used instead of the Au-cone in order to prevent a huge X-ray and γn-neutron noise, and to decrease a hot electron loss in the cone. However the pre-formed plasma grows quickly because the DLC-cone consists of low-Z material. Au-coating on inner side of the DLC-cone has been performed in order to reduce the expansion of the pre-formed plasma. The DLC-cone has also the merit in that the interaction between laser and cone can be observed.

In the integrated experiments, four targets of the stan-

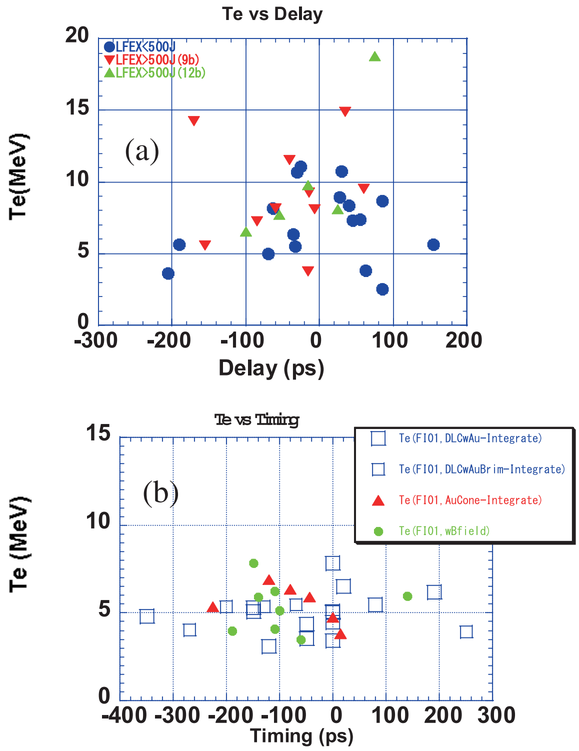

Fig. 3 The implosion timing dependence of T_{eff}. The horizontal axis means the deviation between the maximum compression time of the core and the LFEX injection time. (a) in FG02, (b) in FI01.

dard Au-cone shell, DLC-cone shell, open hole-cone shell and open hole-shell have been tested. In the previous experimental series FG02, the dependence between T_{eff} and the imploding timing (deviation between the imploding time and the LFEX laser injection time) has been plotted as shown in Fig. 3 (a). Maximum T_{eff} could be observed near the implosion time (= imploding timing 0). The residual ω component from the imploding 2ω laser (GXII) may have irradiated the inner wall of the cone. In FI01, T_{eff} can be reduced by elimination of the residual ω component using a mechanical shutter as shown in Fig. 3 (b). However T_{eff} seems to be still higher around the implosion time. The reason is that the lower component of the hot electrons are dissipated in the imploded core. This phenomenon is remarkable in the DLC-cone shell rather than in the Au-cone shell because the lower component of the hot electrons is already lost in the Au-cone itself. Therefore T_{eff} becomes higher.

In FI01, we can suppress the pre-formed plasma scale length within 30 μm (estimated from Phukov scaling) by elimination of the pre-pulse. T_{eff} can be reduce to be 5 MeV in a DLC-cone shell and 6 MeV in an Au-cone shell as shown in Fig. 2. The electron flux in the DLC-cone is almost the same as that in the Au-cone. T_{eff} in an integrated target seems to be determined by the cone shape because T_{eff} in integrated target is almost the same as in the cone only.

In integrated experiments, DD neutrons are measured by MANDALA. The neutron yield in the Au-cone shell is higher than that in the DLC-cone shell. The neutron yield has a strong positive dependence on the imploding laser power. The large imploding laser power produces the high imploding density core. At the beginning, we expected that the lower component of the hot electrons can give their energies to the core in the DLC-cone. However those facts mean that the imploding core in FI01 couples better with the higher energy electrons than we expected. The neutron source region is localized around the core center [17]. The lower component of the hot electrons may heat only the surrounding region of the core but cannot produce neutrons because the electron to ion energy transfer is small due to the low plasma density in the surrounding region.

3.3 External magnetic field application

In integrated experiments, 9 beams out of GXII 12 beams are used for implosion. The external magnetic field (B_{ext}) can be induced by the residual 3 beams of the laser [18]. The laser irradiates the parallel plates with a one turn coil in front of the cone. The magnetic field of several hundred Tesla can be easily obtained in the one turn coil. Here the magnetic field line is along the LFEX laser axis because the space to put all devices is limited. The magnetic field compression by implosion can be expected if the magnetic field is created in a shell before implosion. Therefore the hot electrons which are trapped on the magnetic line can be expected to be guided toward the imploded core.

In integrated experiments, the hot electron spectra with and without B_{ext} are shown in Fig. 4 (a). T_{eff} and the hot electron flux as a function of the LFEX laser intensity are shown in Figs. 4 (b) and (c), respectively. The hot electron flux remarkably increases when B_{ext} is applied although T_{eff} becomes slightly low. The increase of the flux in ESM cannot be explained by the hot electrons convergence due to the magnetic field. The hot electrons convergence due to the magnetic field occurs only around a narrow region (<1 mm) around the core. The magnetic field is open at the position far from the core. The hot electrons diverge with the original divergence angle and are measured at the ESM position (1 m from the core). Therefore almost the same flux should be observed by the ESM. The increase of flux may be explained by the change of the pre-plasma shape in the magnetic field application [19]. The neutron yield does not change clearly even if B_{ext} is applied. The reason is under consideration.

3.4 Open-hole cone shell

Direct heating of the imploded core has been performed by using the open-hole cone shell in order to minimize the energy loss of the hot electrons in the cone itself [20, 21]. At the beginning, we had worried about the increase of T_{eff} due to the exploding plasma with long scale length from the open hole. However T_{eff} is not so high as

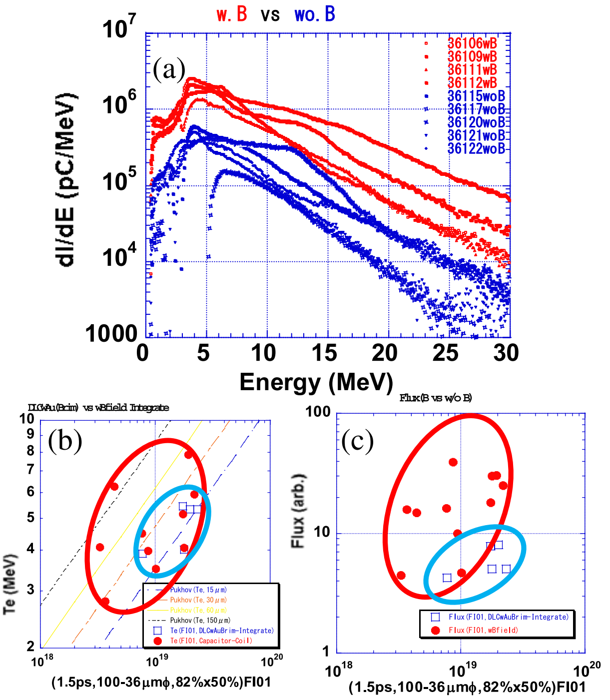

Fig. 4 ESM data with and without B_{ext}. B_{ext} is induced by the laser irradiation to the parallel plates. (a) Hot electron spectra with and without B_{ext}, (b) The laser intensity dependence of T_{eff}, (c) The laser intensity dependence of the hot electron flux.

shown in Fig. 2 and high neutron yield can be obtained. The reason for this may be that the pre-formed plasma is created in the inner side of the imploding shell (because there is no tip of the cone), the pre-formed plasma is shortened by the shell implosion and the scale length remains short because the spouting plasma from the open hole is too dense. Actually the LFEX laser can reach the imploded core according to the MIXS image. Although the neutron yield increases, the neutron energy is shifted from 2.45 MeV (thermal DD neutron) because the accelerated deuterium beam is also contained. The beam may be accelerated in the spouted plasma from the imploded core by the ponderomotive force of the LFEX. The effective core heating can be expected because the stopping range of the accelerated deuterium ion is too short.

4. Summary

The most suitable target for FI can be sought by comparison of the spectra between varied targets using ESM. Generally T_{eff} is low when the target Z is large. However T_{eff} in a copper target may be much higher than T_{eff} in aluminum one due to the contamination of the water on the copper surface.

We compare T_{eff} in the cone irradiated by the LFEX laser with T_{eff} in the plate. T_{eff} in cone is obviously higher than T_{eff} in the plate due to the geometrical effect. In FI01, T_{eff} can be reduced by elimination of the residual ω component in the imploding laser using the mechanical shutter. T_{eff} is high at the implosion time because the lower component of the hot electrons are dissipated in the imploded core. In the integrated experiments, a DLC-cone is used for lower hot electron loss and merits on the diagnostics although the conversion efficiency in a DCL-cone from laser to electron is slightly smaller than that in an Au-cone.

The neutron yield in Au-cone shell is higher than that in DLC-cone shell. T_{eff} in an Au-cone becomes high. The neutron yield can be obtained in higher density. Those facts mean that the imploding core well couples with the higher energy electron rather than the expected optimum energy. By B_{ext} application, the hot electrons are clearly focused. However the neutron yield cannot increase significantly. Direct heating of the imploded core has been performed by using the open-hole cone shell. T_{eff} does not become high and high neutron yield can be obtained. The open-hole cone is another candidate of FI.

Acknowledgements

This work is supported by budgets of NIFS12UJHH003, NIFS10ULHH025, NIFS12KUGK059 and the Grant-in-Aid for Scientific Research (24561028).

[1] T. Yamanaka, private communication.
[2] M. Tabak *et al.*, Phys. Plasmas **1**, 1626 (1994).
[3] R. Kodama *et al.*, Nature **418**, 933 (2002).
[4] T. Jozaki *et al.*, Plasma Phys. Control. Fusion **51**, 014002 (2009).
[5] T. Ozaki *et al.*, J. Phys. Conf. Ser.2, **244**, 022056 (2010).
[6] K. Tanaka *et al.*, Plasma Phys. Control. Fusion **46**, B41 (2004).
[7] H. Azechi *et al.*, J. Phys. **112**, 012002 (2008).
[8] T. Johzaki *et al.*, IFE/P6-01, FEC (2010).
[9] H. Shiraga *et al.*, Rev. Sci. Instrum. **66**, 722 (1995).
[10] N. Izumi *et al.*, Rev. Sci. Instrum. **70**, 1221 (1999).
[11] A. Pukhov *et al.*, Phys. Plasmas **6**, 2847 (1999).
[12] Y. Mishima *et al.*, Rev. Laser Eng. **41**, 49 (2013).
[13] N. Nakanii *et al.*, Appl. Phys. Lett. **93**, 081501 (2008).
[14] H. Sakagami, private communication.
[15] T. Tanimoto *et al.*, Phys. Plasmas **16**, 062703 (2009).
[16] S. Wilks *et al.*, Phys. Rev. Lett. **69**, 1383 (1992).
[17] L. Jarrott *et al.*, Mon. AM, Oral-2, Fast Ignition WS 2012.
[18] S. Fujioka *et al.*, Mon. PM, Oral-5, Fast Ignition WS 2012.
[19] T. Hosogai *et al.*, Phys. Rev. Lett. **97**, 075004 (2006).
[20] Y. Kitagawa *et al.*, Tues. PM, Oral-4, Fast Ignition WS 2012.
[21] A. Sunahara *et al.*, Thur. AM, Oral-2, Fast Ignition WS 2012.